

Neutron Radiative Capture Cross Sections for Na^{23} , Mn^{55} , In^{115} , and Ho^{165} in the Energy Range 1.0 to 19.4 MeV*

H. O. MENLOVE,† K. L. COOP,‡ AND H. A. GRENCHE
Lockheed Palo Alto Research Laboratory, Palo Alto, California

AND

R. SHER
Stanford University, Stanford, California
 (Received 29 June 1967)

Activation cross sections for the $\text{Na}^{23}(n,\gamma)\text{Na}^{24}$, $\text{Mn}^{55}(n,\gamma)\text{Mn}^{56}$, $\text{In}^{115}(n,\gamma)\text{In}^{116m}$, and $\text{Ho}^{165}(n,\gamma)\text{Ho}^{166}$ reactions have been measured at 17 neutron energies between approximately 1.0 and 19.4 MeV. Neutrons were produced by means of the $\text{T}(p,n)\text{He}^3$, $\text{D}(d,n)\text{He}^3$, $\text{Be}^9(\alpha,n)\text{C}^{12}$, and $\text{T}(d,n)\text{He}^4$ reactions using a 3.5-MV Van de Graaff accelerator. The measurements were made relative to the fission cross section of U^{235} for fast neutrons. Thermal irradiations were made in order to obtain cross sections normalized to the thermal-activation cross sections of the irradiated samples and the thermal-fission cross section of U^{235} . The experimental cross-section data for all the isotopes investigated show evidence of a peak in the vicinity of 14 MeV. The measured capture cross sections have been compared with the cross sections predicted by the "direct-capture" reaction theory of Lane and Lynn and by the "semidirect" reaction theory of Brown.

INTRODUCTION

NEUTRON radiative-capture cross-section measurements¹⁻⁵ at 14.5 MeV yield values that are several orders of magnitude larger than the cross sections predicted by the compound-nucleus model of nuclear reactions. Lane and Lynn^{6,7} developed a direct-capture model in an attempt to fit the experimental data in the 5-20-MeV energy range. However, it was shown by Daly *et al.*⁸ that this model predicted cross sections still an order of magnitude smaller than the observed capture cross sections. Brown⁹ and Clement *et al.*¹⁰ have shown that predicted cross sections for "semidirect" or "collective" capture through the giant dipole resonance are in fair agreement with proton radiative-capture data in the 10-20-MeV energy range.

Neutron radiative-capture cross-section data for energies greater than 1 MeV are quite sparse. Johnsrud *et al.*¹¹ measured the neutron capture cross sections of several nuclei at neutron energies up to approximately 6 MeV. Several experimenters¹²⁻¹⁷ have measured capture cross sections at neutron energies extending up to roughly 2-4 MeV. Neutron radiative-capture cross sections at about 14.5 MeV have been measured by Perkin *et al.*,¹ Wille and Fink,² and others. All these experimenters used activation techniques to measure the capture cross sections.

Thus, prior to the measurements carried out in the present experiment, no neutron radiative-capture cross sections had been measured for neutron energies greater than approximately 6 MeV except for the isolated measurements at roughly 14.5 MeV. The purpose of the present experiments was to measure (n,γ) activation cross sections in the neutron energy range from 1.0 to 19.4 MeV. The cross sections of four nuclides, with mass numbers ranging from 23 to 165, were investigated in order to observe the mass dependence of the capture cross sections. These were Na^{23} , Mn^{55} , In^{115} , and Ho^{165} . The choice of these particular nuclides was based primarily on experimental considerations. Perkin *et al.*¹ outline some of the difficulties associated with high-energy (n,γ) cross-section measurements which restrict the choice of target elements.

* This work was supported by the Lockheed Independent Research Program and is based on part of a thesis submitted by H. O. Menlove to Stanford University in partial fulfillment of the requirements for the Ph.D. degree.

† Present address: Los Alamos Scientific Laboratory, University of California, Los Alamos, New Mexico.

‡ Present address: Department of Nuclear Physics, Research School of Physical Sciences, Australian National University, Canberra.

¹ F. L. Perkin, L. P. O'Connor, and R. F. Coleman, *Proc. Phys. Soc. (London)* **72A**, 505 (1958).

² R. G. Wille and R. W. Fink, *Phys. Rev.* **118**, 242 (1960).

³ E. T. Bramlitt and R. W. Fink, *Phys. Rev.* **131**, 2649 (1963).

⁴ J. L. Perkin, *J. Nucl. Energy A/B17*, 349 (1963).

⁵ H. O. Menlove, K. L. Coop, H. A. Grench, and R. Sher, in *Conference on Neutron Cross Section Technology*, edited by P. B. Hemmig, U. S. Atomic Energy Commission Report CONF-660303 (Clearinghouse for Federal Scientific and Technical Information, Springfield, Virginia, 1966), Book 2, p. 746.

⁶ A. M. Lane and J. E. Lynn, in *Proceedings of the Second United Nations International Conference on the Peaceful Uses of Atomic Energy* (United Nations, Geneva, 1958), Vol. 15, Paper P/4.

⁷ A. M. Lane, *Nucl. Phys.* **11**, 625 (1959).

⁸ P. J. Daly, J. R. Rook, and P. E. Hodgson, *Nucl. Phys.* **56**, 331 (1964).

⁹ G. E. Brown, *Nucl. Phys.* **57**, 339 (1964).

¹⁰ C. F. Clement, A. M. Lane, and J. R. Rook, *Nucl. Phys.* **66**, 273 (1965); **66**, 293 (1965).

¹¹ A. E. Johnsrud, M. G. Silbert, and H. H. Barschall, *Phys. Rev.* **116**, 927 (1959).

¹² J. A. Miskel, K. V. Marsh, M. Lindner, and R. J. Nagle, *Phys. Rev.* **128**, 2717 (1962).

¹³ S. A. Cox, *Phys. Rev.* **133**, B378 (1964).

¹⁴ G. Calvi, R. Potenza, R. Ricamo, and D. Vinciguerra, *Nucl. Phys.* **39**, 621 (1962).

¹⁵ Yu. Ya. Stavitskii and V. A. Tolstikov, *At. Energ. (USSR)* **10**, 508 (1961).

¹⁶ A. I. Leipunsky *et al.*, in *Proceedings of the Second United Nations International Conference on the Peaceful Uses of Atomic Energy* (United Nations, Geneva, 1958), Vol. 15, Paper P/2219.

¹⁷ M. V. Pasechnik *et al.*, in *Proceedings of the Second United Nations International Conference on the Peaceful Uses of Atomic Energy* (United Nations, Geneva, 1958), Vol. 15, Paper P/2030.

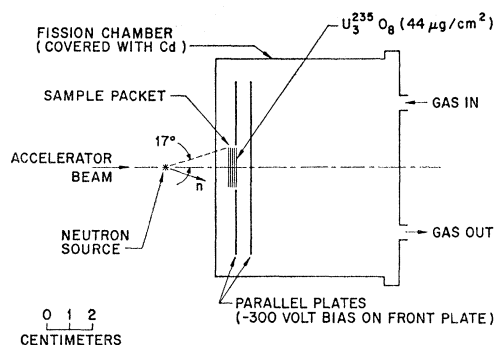


FIG. 1. Schematic drawing of fission chamber and geometry for the fast-neutron irradiations.

Activation techniques were used to determine the number of interactions occurring in the samples during the neutron bombardments. The cross sections were determined relative to the fission cross section of U^{235} . These measured cross sections have been compared with theoretical cross sections calculated by using the simplified "direct-capture" reaction theory of Lane and Lynn⁶ and the "semidirect" reaction theory of Brown.⁹

Activation cross sections for other reactions induced in the target nuclides will be discussed in a companion paper.¹⁸ A more detailed account of all the measurements is also available.¹⁹

EXPERIMENTAL PROCEDURES

Fast-Neutron Activations

Neutrons were produced in the energy region from 1.0 to 2.2 MeV by the $T(p,n)He^3$ reaction, from 3.3 to 6.1 MeV by the $D(d,n)He^3$ reaction, at 8.1 MeV by the $Be^9(\alpha,n)C^{12}$ reaction, and from 13.3 to 19.4 MeV by the $T(d,n)He^4$ reaction. The charged particles were accelerated using the Lockheed 3.5-MV Van de Graaff accelerator. Gas targets of tritium and deuterium were used. The gas was contained in a 3-cm-long gas cell filled to about 0.86-atm pressure. The gas was separated from the accelerator vacuum by a 3.55 mg/cm² Mo foil. The Be target consisted of a thin layer of beryllium which had been evaporated onto a 0.025-cm-thick Ta backing. The Be target was 0.13 MeV thick to 2.5-MeV α particles. The average full neutron-energy spread due to the target thickness and finite sample size was approximately 0.6 MeV.

The samples were prepared for irradiation by forming them into thin disks with diameters of 1.90 cm. In order to obtain Na disks of the size needed for the irradiations, approximately 1 g of NaF powder was pressed in a 1.90-cm-diam die with a pressure of about 30 000 psi. The NaF pellets were then sintered by

heating to a temperature of 700°C for about 4 h in a He-gas atmosphere. The samples of the other three target nuclides were in metallic form. The NaF, Mn, In, and Ho target disks were 0.16, 0.11, 0.013, and 0.051 cm thick, respectively. Before each irradiation, a stack containing disks of the four nuclides was placed between two 0.127-mm-thick Al foils and the sandwich was mounted adjacent to a U^{235} fission foil of the same diameter in a parallel-plate fission counter. All the samples were separated from each other by thin pieces of Mylar tape in order to prevent cross contamination. The Al foils were used in the determination of background effects which will be discussed below. They were also used in connection with the cross-section measurements discussed in the companion paper.¹⁸

A schematic diagram of the fission chamber and the irradiation geometry is given in Fig. 1. The fission chamber was operated as a gas-flow counter at atmospheric pressure using a gas mixture of 97% argon and 3% carbon dioxide. The fission foil consisted of a deposit of U_3O_8 (enriched to 93.17% in U^{235}) on a 0.076-mm-thick Ni backing. The U_3O_8 deposit was sufficiently thin (44 $\mu\text{g}/\text{cm}^2$) that the fission pulses were well separated in energy from the pulses caused by the α -particle background. The fraction of fission pulses occurring under the α -particle background was only about 0.02. The entire chamber was covered with a 0.25-mm-thick layer of cadmium to partially absorb low-energy neutrons.

During the irradiations, the samples were usually located 3.1 cm from the center of the neutron source with their centers on the accelerator-beam axis. At this distance from the source the half-angle subtended by the sample was approximately 17 deg. For the 13.3-MeV neutron irradiation the samples were positioned about 5 cm from the center of the neutron source and at an angle of 124 deg to the accelerator-beam axis. The irradiation periods ranged from 2 to 14 h with beam-current intensities of up to 3 μA on the Mo foil and 4 μA on the Be target. The Be target was gyrotated during the bombardment to reduce local heating.

A "long counter" positioned at 3 m from the neutron source and on the accelerator-beam axis was used to monitor the neutron flux. Time variations in the neutron flux as determined by the "long-counter" count rate were taken into account in the cross-section calculations.

Background-Neutron Determinations

Since the success of (n,γ) cross-section measurements in the high-energy range of this experiment was strongly dependent on correctly taking into account the effects of background neutrons, considerable attention was given to determining these effects and, when possible, reducing them.

Preliminary experiments showed that platinum yielded fewer neutrons when bombarded by 3-MeV deuterons than did gold or tantalum; therefore, plati-

¹⁸ H. O. Menlove, K. L. Coop, H. A. Grench, and R. Sher, following paper, Phys. Rev. 163, 1308 (1967).

¹⁹ H. O. Menlove, K. L. Coop, and H. A. Grench, Lockheed Palo Alto Research Laboratory Report No. 6-76-66-18, 1966 (unpublished).

num was used for the beam collimator and for the beam stopper in the gas cell. The beam stopper and collimator were replaced several times during the experiment in order to prevent excessive deuterium buildup.

Room-Scattered Neutrons

To minimize background-neutron production, the neutron source and irradiation sample were located above a pit covered with a thin Al floor and about 3 m from the nearest wall.

During the irradiations at neutron energies of 1.6, 2.2, 6.1, 8.1, 13.3, 15.0, 18.4, and 19.4 MeV, a Cd-covered sample packet similar to the primary sample packet in the fission chamber was positioned at 90 deg to the accelerator-beam axis and at 1 m from the neutron source. From the activity induced in this packet it was possible to make a correction for room-scattered neutrons from the primary source. A linear interpolation of the measured effect was used to correct the data at the neutron energies where the effect was not measured. Typical values of this correction were 2, 3, 10, and 8% for Na, Mn, In, and Ho, respectively. A measurement of possible spatial variations in this room-scattered-neutron effect was made by irradiating In samples simultaneously at the following positions: 1 m and 90 deg, 1 m and 0 deg; and 0.5 m and 0 deg. It was found that the specific activity induced in each of the In samples from scattered neutrons was the same to within the $\pm 4\%$ counting statistics.

The fission chamber was also operated 1 m from its usual position, and it was observed that the fission-chamber counting rate was less than 1% of its normal rate. Thus, room background was not an important contributor to this rate.

Non-Primary-Source Neutrons

After each irradiation, the tritium or deuterium gas was removed from the gas cell and the cell was filled with hydrogen gas. The fission chamber, containing a new set of samples, was then placed in its normal irradiation position and the preceding bombardment was repeated. In this manner, corrections for activity in the samples produced by neutrons not originating from the desired source reaction could be made. The magnitude of this correction ranged from 0.1 to 29%.

To measure this effect for the $\text{Be}^9(\alpha, n)\text{C}^{12}$ source reaction, the Be target was replaced by a clean Ta backing and bombarded with α particles. The resulting neutron flux was found to be negligible.

Scattered Neutrons from the Target Vicinity

The effects of neutron scattering by the fission chamber were investigated by repeating the cross-section measurements at neutron energies of 1.0, 6.1, and 15.0 MeV with the fission chamber removed. The ratio of the neutron fluxes passing through the samples

with and without the fission chamber present was obtained from the observed activities induced in In and Al in the two cases. Scattered neutrons from the fission chamber were found to affect the measured values of the (n, γ) cross sections by less than 6%.

In order to determine the effect of the sample packet itself on the measurements, all the target samples except indium were removed from the fission chamber, and the irradiations were repeated at neutron energies of 2.2, 4.6, 5.4, 15.0, 17.4, and 18.4 MeV. The same procedure was repeated for the Ho targets at neutron energies of 2.2, 5.4, 15.0, 17.4, and 18.4 MeV and for the Na and Mn targets at a neutron energy of 15.0 MeV. The Na and Mn samples by themselves were remeasured at only one neutron energy since the effects of the other samples were found to be negligible in the Na and Mn cross-section calculations. On the other hand, scattered neutrons from the sample packet raised the measured values of the (n, γ) cross section of In by amounts ranging from 5 to 18% at the various neutron energies at which this measurement was made. The measured cross sections for Ho were found to be increased by from 1 to 27% by this effect. The measured correction was adjusted to account for the remaining scattering of neutrons from the target sample and its thin Cd cover. This self-scattering effect was assumed to be proportional to the fractional mass of material remaining, and the correction was at most 6%.

In order to determine the effect of neutrons which were scattered by the gas-cell assembly, two assembly units similar to the one used in the experiment were placed beside the gas cell. Irradiations with 15.0-MeV neutrons were performed both with and without the extra assemblies, and it was found that the fission count rate increased when the extra units were present by about 2%, which was just outside the uncertainty arising from counting statistics.

Target-Sample Counting

After the irradiations, the activated samples were counted on four NaI(Tl) crystals which were coupled to four 100-channel sections of a 400-channel pulse-height analyzer. The activated NaF disks were counted on the face of a cylindrical 4 in. \times 4 in. NaI(Tl) crystal which was covered with a 0.10-cm-thick Lucite shield. For activations carried out at neutron energies greater than 8 MeV, the decay of Na^{24} was not followed for the first 5 h after the irradiation because of the presence of short-lived activities. The activated Mn disks were counted on top of a cylindrical 3 in. \times 3 in. NaI(Tl) crystal which was covered with a 0.05-cm-thick Lucite shield, and the activated In samples were counted on top of a 2 in. \times 2 in. NaI(Tl) crystal. The Ho samples were counted on the face of a cylindrical 1.75 in. diam \times 0.25 in. NaI(Tl) crystal. This crystal had a thin Al window so that β rays from the Ho^{166} (27 h) activity could be detected with good efficiency. The decay of

TABLE I. Information concerning the investigated nuclides.

Reaction	Thermal activation cross section (b)	Half-life	Counting interval (keV)
$\text{Na}^{23}(n,\gamma)\text{Na}^{24}$	0.534 ± 0.005	15.05 h	1240-1520, 2630-2880
$\text{Mn}^{55}(n,\gamma)\text{Mn}^{56}$	13.3 ± 0.1	2.58 h	720-960, 1650-2270
$\text{In}^{115}(n,\gamma)\text{In}^{116m}$	157 ± 4	54.13 min	1010-1365
$\text{Ho}^{165}(n,\gamma)\text{Ho}^{166}$	64 ± 10	27.0 h	>80

Ho^{166} was not followed for the first 24 h after the irradiation because of the presence of short-lived activities.

Table I lists the reactions for which cross sections were measured, the half-lives²⁰ of the induced activities, and the energy intervals that were analyzed in order to determine the number of interactions that occurred during the neutron irradiations. The pulse-height spectra from each sample were collected for a period of several half-lives, and the decay of the selected portions of the spectrum was analyzed by means of a least-squares exponential-decay computer program.

Thermal Neutron Irradiations

As will be explained below, thermal-neutron irradiations were performed in order to normalize the relative fast-neutron cross sections as a function of energy. For an irradiation of length t by a constant neutron flux, the activation cross section σ of a nucleus can be expressed in terms of the $\text{U}^{235}(n,f)$ cross section σ_U as

$$\sigma = \frac{R\epsilon_U N_U \sigma_U}{R_U \epsilon_N [1 - \exp(-\lambda t)]}$$

In the formula R is the counting rate of the sample at the end of the irradiation, ϵ the counting efficiency (the ratio of the counting rate to the disintegration rate), N the number of atoms in the sample, and λ the decay constant. The symbols subscripted U are analogous except that R_U is the observed counting rate in the fission chamber during the irradiation. Since N , λ , and σ_U were known, and R and R_U were measured for each fast-neutron irradiation, the desired cross section could be obtained if the factor $\epsilon_U N_U / \epsilon$ were known. This factor was determined in two ways. The primary method consisted of using the results of thermal-neutron bombardments. Since σ and σ_U were both known for thermal energy and all other factors appearing in the formula were determined experimentally, the equation could be solved for $\epsilon_U N_U / \epsilon$.

A secondary method was also used to normalize the relative cross sections of Na^{23} , Mn^{55} , and In^{115} . This method was a two-step process, the first step consisting of a determination of $\epsilon_U N_U / \epsilon_{\text{Au}}$ at thermal energy. In this case gold was the target sample, and ϵ_{Au} refers to the efficiency for counting the γ rays emitted by Au^{198} .

In the second step, the ratios $\epsilon_{\text{Au}} / \epsilon$ for the three nuclides whose cross sections were normalized by this procedure were determined by a series of crystal-efficiency calibration experiments. The desired quantity, $\epsilon_U N_U / \epsilon$, could then be obtained for each nuclide from the known quantities $\epsilon_U N_U / \epsilon_{\text{Au}}$ and $\epsilon_{\text{Au}} / \epsilon$. The fast-neutron cross sections obtained using this method ultimately depend on σ_{Au} and σ_U for thermal neutrons, but not on the thermal cross sections of Na^{23} , Mn^{55} , or In^{115} .

The thermal-neutron irradiations took place in the thermal column of the Stanford University research reactor. The neutrons in the thermal column were collimated by means of Cd shielding before they entered the fission chamber. Because of the sizeable thermal-neutron absorption cross section of the target samples, only one sample at a time was placed in the fission chamber during the thermal irradiations. In order to measure the neutron absorption in the samples, a 0.025-mm-thick Au foil was placed on each side of the sample. A stack of these Au foils was placed in the same thermal flux in order to measure the neutron absorption in the gold. The absorption was found to be about 1% for a 0.025-mm-thick Au foil. The irradiations were repeated with cadmium covering the collimation aperture in order to determine the effect of epi-cadmium neutrons. The contribution to the activity of the samples and to the fission count rate from epi-cadmium neutrons was found to be less than 0.8% of the activity produced by the thermal neutrons.

The thermal-neutron irradiation of the fission chamber and gold foil to determine $\epsilon_U N_U / \epsilon_{\text{Au}}$ was performed before the start of the fast-neutron irradiations. This experiment was repeated about one year later at the completion of the fast-neutron irradiations and the results agreed to within 0.5%.

As indicated previously, the secondary method of normalizing the relative cross sections required a knowledge of the ratio $\epsilon_{\text{Au}} / \epsilon$ for the Na^{24} , Mn^{56} , and In^{116m} activities. Absolute efficiencies were not required. A crystal-calibration curve had been previously obtained²¹ for point sources 15.2 cm above the 4×4 in. NaI(Tl) crystal which was covered by a 0.75 g/cm² β -ray absorber. Supplementary experiments, therefore, were performed for each of the samples to relate the counting rate in the usual close geometry on the crystal normally used to the rate in the calibration geometry. Other supplementary measurements were made at the 15.2-cm position in order to correct for the effects of γ -ray self-absorption in the sample, γ -ray summing, and the finite sample dimensions. None of these corrections was more than 5%. Gaussian curves were fit to the results in the 15.2-cm geometry for the 2.75-, 0.835-, 1.29-, and 0.412-MeV photopeaks of Na^{24} , Mn^{56} , In^{116m} , and Au^{198} , respectively, to obtain the emission rates of these γ rays. The number of these γ rays per

²⁰ *Nuclear Data Sheets*, compiled by K. Way *et al.* (Printing and Publishing Office, National Academy of Sciences-National Research Council, Washington, D. C., 1958-64).

²¹ K. L. Coop and H. A. Grench, *Nucl. Instr. Methods* **36**, 339 (1965).

TABLE II. The (n,γ) activation-cross-section results.

Neutron energy ^a (MeV)	One-half full energy spread (MeV)	$U^{235}(n,f)^b$ $\sigma(n,f)$ (b)	$Na^{23}(n,\gamma)Na^{24}$ $\sigma(n,\gamma)$ (mb)	$Mn^{55}(n,\gamma)Mn^{56}$ $\sigma(n,\gamma)$ (mb)	$In^{115}(n,\gamma)In^{116m}$ $\sigma(n,\gamma)$ (mb)	$Ho^{165}(n,\gamma)Ho^{166}$ $\sigma(n,\gamma)$ (mb)
0.97	0.10	1.22	0.255±0.019 ^c	2.80 ±0.22 ^c	205 ±18 ^c	124 ±21 ^c
1.56	0.12	1.26	0.191±0.015	1.94 ±0.15	157 ±14	83 ±14
2.15	0.13	1.31	0.210±0.016	1.89 ±0.14	120 ±10	48.3 ± 8.4
3.27	0.52	1.28	0.198±0.019	1.46 ±0.12	40.3 ± 3.7	23.4 ± 4.2
3.57	0.29	1.27	0.163±0.017	1.36 ±0.10	31.1 ± 2.9	19.3 ± 3.4
4.00	0.24	1.24	0.170±0.014	1.24 ±0.09	21.1 ± 2.1	13.7 ± 2.4
4.58	0.23	1.20	0.158±0.013	1.09 ±0.08	14.7 ± 1.5	9.89± 1.78
5.39	0.25	1.16	0.169±0.016	0.964±0.088	9.89± 1.07	7.40± 1.43
6.13	0.28	1.28	0.169±0.016	0.855±0.078	7.28± 0.90	6.55± 1.31
8.06	0.14	1.80	0.171±0.015	0.695±0.063	5.83± 0.98	6.70± 1.54
13.28	0.61	1.95	0.221±0.024	0.907±0.088	6.25± 1.08	7.97± 1.81
14.96	0.87	2.25	0.249±0.023	0.889±0.081	5.97± 0.81	6.87± 1.44
15.82	0.45	2.33	0.240±0.024	0.843±0.077	6.20± 0.82	6.81± 1.42
16.52	0.35	2.35	0.229±0.021	0.757±0.069	6.41± 0.89	7.61± 1.59
17.35	0.32	2.30	0.194±0.018	0.705±0.071	5.82± 0.83	6.27± 1.35
18.44	0.33	2.18	0.177±0.032	0.580±0.055	6.61± 1.18	6.92± 1.44
19.39	0.35	2.11	0.195±0.021	0.472±0.048	6.86± 1.03	6.26± 1.42

^a Laboratory system.^b Fission cross sections taken from Ref. 25.^c Uncertainty in absolute value of the cross section.

decay²⁰ of the nuclide was taken to be 1.00, 0.99, 0.82, and 0.96 for Na²⁴, Mn⁵⁶, In^{116m}, and Au¹⁹⁸, respectively.

RESULTS AND DISCUSSION

Experimental Results

The measurements were corrected to take into account the effects of room-scattered neutrons, neutrons scattered from the fission chamber and the sample packet, and neutrons from reactions other than the primary neutron-source reaction; differences in the neutron flux incident on the samples and on the U²³⁵ foil; time variations in the neutron flux during the irradiation; and the presence of the second neutron group from the Be⁹(α,n)C¹² reaction. The intensity of the excited-state group of neutrons relative to the ground-state group in the Be⁹(α,n)C¹² reaction was taken from the measurements of Chase *et al.*²² This second-neutron-group correction was only needed at 8.1 MeV and it changed the uncorrected cross sections by 4 to 38%. The thermal cross sections were corrected according to the procedure of Westcott^{23,24} for the effects of non-1/ v cross-section behavior and nonthermal neutrons. The effect of this correction on the cross sections ranged from 2.6 to 4.8%.

Uncertainties enter into the present cross-section calculations from a large number of sources and usually these errors vary with the neutron energy and target nuclide. Uncertainties in the corrections for background neutrons generally dominate the uncertainty in the final cross-section value. The following sources of error affect the relative cross-section values (all quoted

uncertainties are in terms of standard deviation): (a) counting statistics and electronic gain shifts (± 1 –10%), (b) room-scattered neutrons (± 0.3 –7%), (c) neutrons scattered from the sample packet and its immediate vicinity (± 2 –13%), (d) the ratio of the intensity of the second neutron group from the Be⁹(α,n)C¹² reaction to that of the higher-energy group (± 0.4 –6%), and (e) the shape of the U²³⁵ fission cross section (<5%). The sources of error which pertain equally to all measurements for a particular nuclide, regardless of energy, and hence, do not affect the relative cross sections are as follows: (a) activation and fission cross sections for thermal neutrons (± 0.2 –16%), (b) the (n,f) cross section of U²³⁵ (± 5 % for the neutron energy range of 1 to 5 MeV and ± 7 % for the neutron energy range of 5 to 19.5 MeV), and (c) the position of the samples relative to the fission foil (± 0.5 –1.5%). The total error in each cross section was obtained by combining the contributing errors by quadratures.

The results of the present cross-section measurements are given in Figs. 2–5 and Table II. These results were obtained relative to the U²³⁵ fission cross section²⁵ for fast neutrons. The cross sections were normalized to the thermal-fission cross section²⁶ of U²³⁵ (577.1 b) and to the thermal-activation cross sections²⁷ of the target nuclides which are given in Table I. Table II lists the average neutron energy in the laboratory system and the value of the U²³⁵ fission cross section which was used in the calculations. For each irradiation, the average neutron energy was obtained by using a computer code which

²⁵ *Neutron Cross Sections*, compiled by J. R. Stehn *et al.* Brookhaven National Laboratory Report No. 325 (U. S. Government Printing and Publishing Office, Washington, D. C., 1958), 2nd ed., Suppl. 2, Vol. III.

²⁶ R. Sher and J. Felberbaum, Brookhaven National Laboratory Report No. BNL-918 (unpublished).

²⁷ *Neutron Cross Sections*, compiled by J. R. Stehn *et al.* Brookhaven National Laboratory Report No. 325 (U. S. Government Printing and Publishing Office, Washington, D. C., 1958), 2nd ed., Suppl. 2, Vol. I, IIA, and IIB.

²² L. F. Chase, Jr., R. G. Johnson, R. V. Smith, F. J. Vaughn, and M. Walt, Lockheed Missiles and Space Division Report No. AFSWC-TR-61-15, 1961 (unpublished).

²³ C. H. Westcott, Atomic Energy of Canada Limited Report No. CRRP-662, 1962 (unpublished).

²⁴ C. H. Westcott, Atomic Energy of Canada Limited Report No. CRRP-680, 1957 (unpublished).

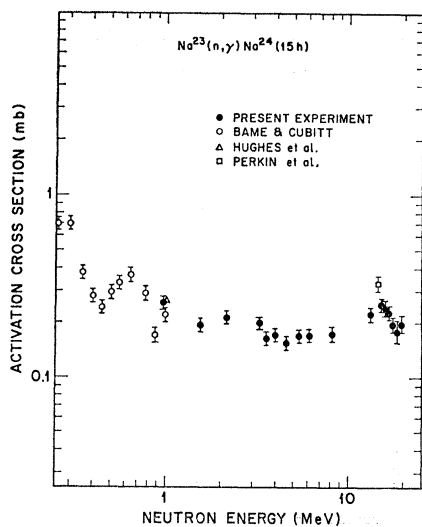


FIG. 2. The $\text{Na}^{23}(n,\gamma)\text{Na}^{24}(15\text{ h})$ activation cross section.

takes into account the target thickness, the irradiation geometry, and the dependence of the neutron production reaction on energy and angle. The energy resolution given in Table II corresponds to one-half the full neutron energy spread.

As described above, the capture cross sections of Na^{23} , Mn^{55} , and In^{115} were also obtained by means of relative γ -ray counting techniques. The cross sections obtained from the relative γ -counting method were 2.3, 3.3, and 5.9% lower than those obtained from the thermal-normalization method for Na^{23} , Mn^{55} , and In^{115} , respectively. Ho^{165} was not included in this method, since the decay of $\text{Ho}^{166}(27\text{ h})$ does not contain a γ ray of sufficient intensity to make the method practical. The agreement between the two methods of determining the cross sections is quite good, and in all cases the difference can be accounted for by the uncertainties in the two methods. The (n,γ) cross sections listed in Table II were obtained using the thermal normalization method, since that method yields results with smaller uncertainties. Also, if more accurate values of the thermal cross sections become available, the fast-neutron cross sections can easily be renormalized to the new thermal values.

Comparison with Other Measurements

Neutron-capture cross-section results obtained by other investigators are shown in Figs. 2-5 for comparison with the present results. Johnsrud *et al.*¹¹ calculated their activation cross sections using a U^{235} fission cross section of 584 b for thermal neutrons and the values given by Allen and Henkel²⁸ for fast neutrons. Where appropriate, we have adjusted Johnsrud's (n,γ) cross sections to correspond to more recent values^{25,26} of the

U^{235} fission cross section. This adjustment never exceeded 9%. The measurements of Leipunsky *et al.*¹⁶ were made relative to the (n,γ) cross section of I^{127} . The cross-section results of Perkin *et al.*¹ at 14.5 MeV were obtained by absolute β -ray counting techniques and the neutron flux was measured by counting the α particles associated with the $\text{T}(d,n)\text{He}^4$ reaction.

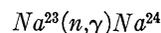


Figure 2 shows the comparison of the Na^{23} cross-section results of the present experiment with those of

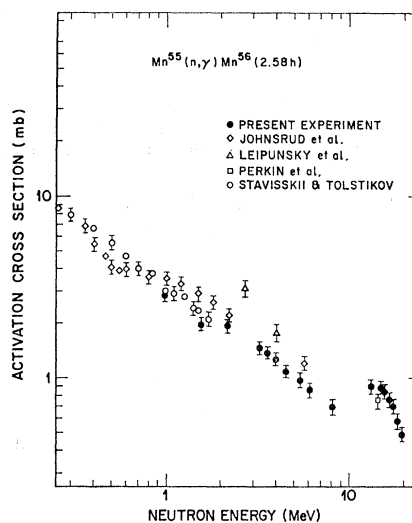


FIG. 3. The $\text{Mn}^{55}(n,\gamma)\text{Mn}^{56}(2.58\text{ h})$ activation cross section.

other investigators. The 1-MeV measurement of this experiment can be compared with the results of Bame and Cubitt,²⁹ which have been adjusted to more recent values of the U^{235} fission cross section. Their $0.22\text{ mb} \pm 8\%$ cross section at 1 MeV is about 15% lower than the present result of $0.26\text{ mb} \pm 8\%$. Considering the standard deviations of the two experiments, the agreement is satisfactory. When the (n,γ) cross section of Hughes *et al.*³⁰ for fission neutrons with an effective energy of 1 MeV is renormalized to a more recent value of the Na^{23} thermal-activation cross section, the result is 0.28 mb. When the cross-section results of the present experiment are averaged over a fission spectrum, the result is 0.21 mb. Leipunsky *et al.*¹⁶ measured upper limits for the (n,γ) cross section of Na^{23} to be 0.23 mb at 2.7 MeV and 0.12 mb at 4 MeV. The Na^{23} cross-section measurement of Perkin *et al.*¹ at 14.5 MeV is $0.33\text{ mb} \pm 10\%$, which is 32% higher than the $0.25\text{ mb} \pm 10\%$ result of the present experiment. The combined errors given in the two experiments cannot account for the discrepancy.

²⁹ S. J. Bame, Jr. and R. L. Cubitt, *Phys. Rev.* **113**, 256 (1959).

²⁸ W. D. Allen and R. L. Henkel, *Progress in Nuclear Energy*, (Pergamon Press, Inc., New York, 1958), Ser. I, Vol. II.

³⁰ D. J. Hughes, R. C. Garth, and J. S. Levin, *Phys. Rev.* **91**, 1423 (1953).

$$Mn^{55}(n,\gamma)Mn^{56}$$

Figure 3 shows the present Mn^{55} results compared with other measurements of the capture cross section. The shape of the present cross-section curve parallels the measurements of Johnsrud *et al.*¹¹; however, Johnsrud's results are roughly 20% higher than those of the present experiment. This discrepancy is slightly larger than the combined error of 16% for the two results. The cross-section measurements of Staviskii and Tolstikov¹⁵ have been adjusted to correspond to more recent measurements of the U^{235} fission cross section, and the results agree very well ($\pm 5\%$) with the present measurements. The two cross-section measurements by Leipunsky *et al.*¹⁶ are roughly a factor of 1.5 above the present results. This discrepancy cannot be accounted for by the stated uncertainties of $\pm 10\%$ for Leipunsky's measurements and $\pm 8\%$ for the present results. The capture cross section of Mn^{55} measured by Perkin *et al.*¹ at 14.5 MeV is 0.76 mb $\pm 10\%$, which is 15% lower than the 0.89 mb $\pm 9\%$ result of the present experiment. It is somewhat surprising that their Mn measurement is lower than the present results while their Na measurement is substantially higher than the

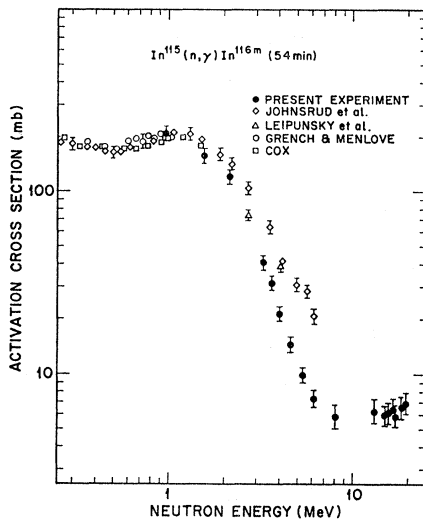


FIG. 4. The $In^{115}(n,\gamma)In^{116m}$ (54 min) activation cross section.

present results, since most of the systematic errors would have the same effect on both nuclides.

$$In^{115}(n,\gamma)In^{116m}$$

Figure 4 shows the present In^{115} capture cross sections compared with the results of other experiments. At 1 MeV the present result agrees very well with the results of Cox,¹³ Grench and Menlove (values revised from preliminary results given in Refs. 27 and 31), and Johnsrud *et al.*¹¹ The measurement of Leipunsky

¹³H. A. Grench and H. O. Menlove, Bull. Am. Phys. Soc. 8, 478 (1963).

*et al.*¹⁶ at 2.7 MeV agrees well with the present results; however, Leipunsky's measurement at 4 MeV is roughly a factor of 1.7 higher than the present results.

A possible explanation for the discrepancy in shape between the present results and those of Johnsrud is given in the following section.

$$Ho^{165}(n,\gamma)Ho^{166}$$

Figure 5 shows the present Ho^{165} measurements compared with the results of Johnsrud *et al.*¹¹ and Perkin *et al.*¹ Perkin's 9.45-mb result at 14.5 MeV is roughly 27% higher than the present measurement. This discrepancy is about equal to the combined uncertainty of the two experiments.

For In^{115} and Ho^{165} , the present data agree very well with Johnsrud's measurements at 1 MeV. However, as the neutron energy increases, our cross-section results drop below the values given by Johnsrud *et al.* At approximately 6 MeV, the two curves differ by about a factor of 2. Some of this discrepancy may be due to the effects of room-scattered neutrons. The sharp decline of the (n,γ) cross sections of these two nuclides in the 1–6 MeV energy region makes them especially vulnerable to the effects of scattered neutrons. Johnsrud *et al.* estimated the effect of room-scattered background neutrons by repeating some of the activations at distances greater than normal from the neutron source and assuming that the direct neutron flux varied inversely with the square of the distance. His corrections for room-scattered background neutrons were stated to be always less than 8%. In the present experiment a background sample packet, similar to the primary sample packet, was located 1 m away from the neutron source. For the 6-MeV irradiation, the ratio of the activity in this packet to that in the primary packet amounted to 5.8% for In^{115} and 2.8% for Ho^{165} . The distance from the sample to the neutron source was 3.1

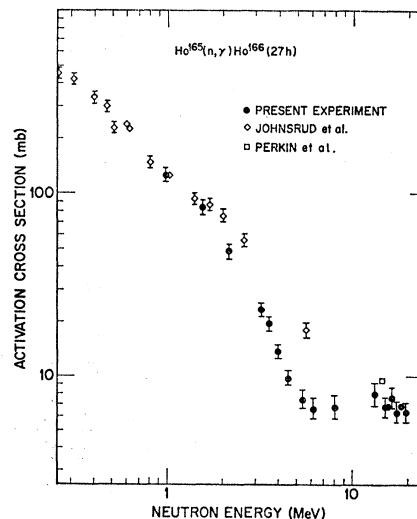


FIG. 5. The $Ho^{165}(n,\gamma)Ho^{166}$ (27 h) activation cross section.

cm compared with 8 cm in Johnsrud's experiment. If an 8-cm source-to-sample distance had been used in the present experiment, the effect of room-scattered background neutrons would have been approximately 38% for In¹¹⁵ and 19% for Ho¹⁶⁵. Also, it was found that if the Cd covers of the samples were removed, this background effect increased by approximately a factor of 4. Thus, it is possible that Johnsrud did not make a sufficient correction for the effects of scattered neutrons.

DISCUSSION AND COMPARISON WITH THEORY

Radiative-capture cross sections are predicted fairly well by the compound-nucleus reaction mechanism for neutron energies up to about 4 MeV. At higher energies, the cross sections for radiative capture via compound-nucleus formation are strongly reduced due to competition from other modes of decay. According to Lane and Lynn,⁶ the compound-nucleus theory predicts that the radiative-capture cross sections will decrease by 2 to 5 orders of magnitude as the neutron energy goes from 1–14 MeV. However, measurements^{1–5} in this energy range show that the capture cross sections decrease by only a factor of 20 or less. Consequently, for neutron energies of about 5–10 MeV (depending on the specific nucleus), it is likely that the radiative-capture cross sections are dominated by a reaction mechanism which is not subject to this competition.

Direct Capture

In contrast to this two-stage capture process of the compound-nucleus model, several authors^{6,32,33} have suggested a one-stage or direct-capture mechanism in which the incident particle is directly captured into a bound single-particle state of the target nucleus which acts as the core.

For the special case of neutron bombardment and a square-well potential, Lane and Lynn⁶ showed that the direct-capture cross section is roughly given by the expression

$$\sigma(n,\gamma) \approx 6 \left(\frac{Z}{A} \right)^2 \frac{R^4 (E_n)^{1/2} E_\gamma^3 \times 10^{-10}}{2 + 0.5E_n + [16.8(E_n)^{1/2}/R]} \text{ barns}, \quad (1)$$

where Z and A are the charge and mass number, R is the nuclear radius in fermis, E_n is the neutron energy in MeV, and E_γ is the radiated-photon energy in MeV. The emitted-photon energies range from E_n to $E_n + B$, where B is the binding energy of the neutron. The quantity E_γ was taken as $E_n + B/2$ in the present calculations.

In arriving at Eq. (1), Lane and Lynn included contributions to the electric-dipole transition-matrix elements only for distances less than the nuclear radius. However, in a later publication,³⁴ they showed that at

14 MeV the cross sections predicted by Eq. (1) are increased by roughly a factor of 4 if contributions to the electric-dipole integral for radial distances $r > R$ are not neglected. They also conjectured that the cross section would be further increased if a more realistic rounded potential were used instead of their square-well potential.

In a subsequent article, Daly, Rook, and Hodgson⁸ showed that the rounded potential of a Saxon-Woods form decreases the direct-capture cross section from the calculation given by Lane and Lynn. For 14-MeV neutrons and heavy nuclides ($A > 200$), the square-well calculations were reduced by roughly a factor of 8 when the Saxon-Woods potential was used. This reduction in cross section is primarily due to a partial cancellation of the interior ($r < R$) and the exterior ($r > R$) contributions to the electric-dipole integral.

Recently, Gutfreund and Rakavy³⁵ have extended the direct-capture model of Daly *et al.* to include the spin-orbit interaction in the nuclear potential for the incoming particle. For energies below 20 MeV, Gutfreund and Rakavy found that the calculated cross sections were quite sensitive to variations in the optical-potential parameters, but the parameters had to be shifted outside the limits indicated by scattering experiments in order to get agreement with (p,γ) cross-section measurements.

Collective Capture

Brown⁹ and Clement *et al.*¹⁰ have shown that in addition to direct capture, "semidirect" or "collective" capture through the giant dipole states of nuclei is important in the energy region of 10–20 MeV. For energies near the giant dipole resonance (≈ 14 MeV), this collective mode of capture was found to be completely dominant. It was assumed that the charge and mass densities of the nucleus are capable of shape oscillations in various multipole modes, and the nuclear potential oscillates in the same modes as these densities. Due to this oscillation of the target nucleus, the incident particle will not experience a spherically symmetric potential as was assumed in Lane and Lynn's previous model, but rather the potential will be slightly deformed. Collective modes of the target nucleus can be excited through the interaction with the incident particle. For incident energies near the giant dipole resonance, the incident nucleon and the target nucleus interact to give an intermediate state in which the former is in a bound state and the latter is excited to its giant dipole state. The giant dipole state then decays by γ -ray emission, and enhancement over the values obtained in previous calculations⁸ is expected from the collective nature of the dipole state. Typically, this effect increases the calculated cross section by roughly an order of magnitude for neutron energies near 14 MeV.

³² B. L. Cohen, Phys. Rev. **100**, 206 (1955).

³³ F. Beck, Nucl. Phys. **9**, 140 (1958/1959).

³⁴ A. M. Lane and J. E. Lynn, Nucl. Phys. **11**, 646 (1959).

³⁵ H. Gutfreund and G. Rakavy, Nucl. Phys. **79**, 257 (1966).

TABLE III. Parameters used in calculating the enhancement factor F .

Nuclide	E_D^a (MeV)	Γ_D^b (MeV)
Na ²³	19.0	8.0
Mn ⁵⁵	18.0	7.5
In ¹¹⁵	15.0	5.8
Ho ¹⁶⁵	14.5	6.9

^a Position of giant (γ, n) resonance.
^b Width of giant (γ, n) resonance.

Brown⁹ considered the case of photonuclear emission and gave the square of the absorption amplitude as

$$|S_{ab}|^2 \approx \left| 1 + \frac{\Delta E}{E_0 + \hbar\omega - E_D + (i\Gamma_D/2)} \right|^2 \equiv F, \quad (2)$$

where E_D is the peak energy and Γ_D the width of the giant dipole resonance, $E_0 + \hbar\omega$ is the excitation energy of the incident-particle and target-nucleus system which is available for γ emission, and ΔE is the energy shift of the dipole state from some average unperturbed particle-hole energy.³⁶ The first term on the right-hand side of Eq. (2) corresponds to the direct-capture process and the second term, containing the factor ΔE , corresponds to the "semidirect" process which adds to the direct term.

Brown used the enhancement factor given by Eq. (2) to increase the direct-capture cross sections predicted by Daly *et al.* Typical values of Γ_D are 4–8 MeV and of ΔE are 6–8 MeV; hence, the enhancement factor F is of the order of 10 at the giant-dipole resonance energy ($E_0 + \hbar\omega = E_D$).

The values of the parameters E_D and Γ_D used in the calculation of F for the nuclides of this experiment were taken from the results of (γ, n) cross-section measurements.^{37–41} The binding energy of a neutron in its final state was taken to be $B/2$ and ΔE was taken as 7 MeV. Table III lists the (γ, n) resonance parameters used in the calculations of F .

Comparison with Measurements

It can be seen in Figs. 2–5 that the radiative-capture cross sections do not continue the rapid decrease with increasing neutron energy predicted by the compound-nucleus model of nuclear reactions.^{6,7} For the nuclides involved in this experiment, it is observed that the (n, γ) cross sections start to level off or rise at a neutron

³⁶ G. E. Brown, *Unified Theory of Nuclear Models* (North-Holland Publishing Company, Amsterdam, 1964).

³⁷ R. Montalbetti, L. Katz, and J. Goldemberg, *Phys. Rev.* **91**, 659 (1953).

³⁸ S. Costa, F. Ferrero, S. Ferroni, B. Minetti, C. Molino, and R. Malvano, *Phys. Letters* **6**, 226 (1963).

³⁹ R. W. Parsons, *Can. J. Phys.* **37**, 1344 (1959).

⁴⁰ E. G. Fuller and E. Hayward, *Nucl. Phys.* **30**, 613 (1962).

⁴¹ R. L. Bramblett, J. T. Caldwell, G. F. Auchampaugh, and S. C. Fultz, *Phys. Rev.* **129**, 2723 (1963).

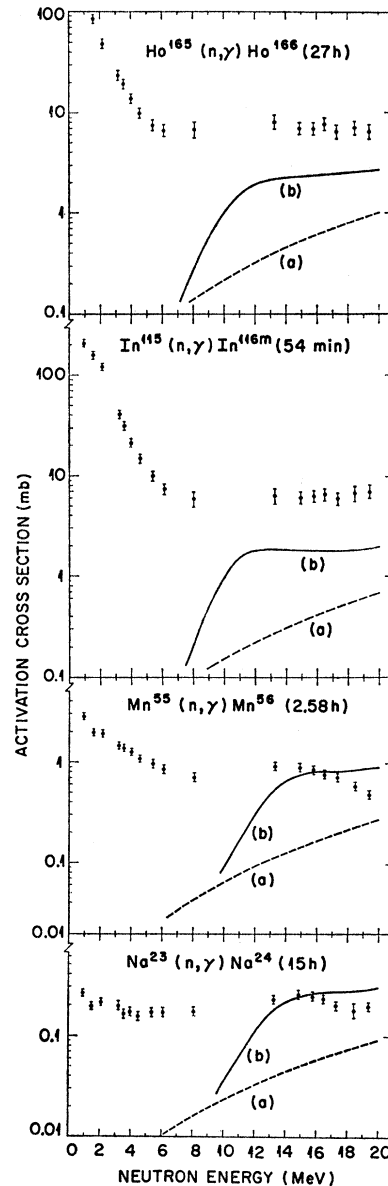


FIG. 6. The (n, γ) cross-section measurements of the present experiments compared with the theoretical calculations. The dashed curve (a) corresponds to Lane and Lynn's simplified direct-capture cross sections, and the solid curve (b) corresponds to curve (a) multiplied by Brown's enhancement factor F .

energy of about 6 to 8 MeV. This finding is consistent with the predictions of Lane and Lynn^{6,34} based on their direct-capture model. In addition, the neutron-capture cross sections show evidence of a peak in the experimental data at approximately 14 MeV. This effect is similar to that observed in the proton radiative-capture cross sections measured by Daly and Shaw.⁴² This peak in cross sections at about 14 MeV is consistent with the theoretical predictions of Brown⁹ and Clement *et al.*¹⁰ According to their predictions, "semidirect" or "collec-

⁴² P. J. Daly and P. F. D. Shaw, *Nucl. Phys.* **56**, 322 (1964).

tive" capture through the giant dipole resonance results in a peak in the cross sections at about 15 MeV.

Figure 6 shows the (n,γ) cross-section measurements of this experiment compared with the theoretical predictions of Lane and Lynn⁶ and Brown.⁹ The dashed curve (a) corresponds to Lane and Lynn's simplified direct-capture cross section [Eq. (1)] and the solid curve (b) corresponds to curve (a) multiplied by Brown's enhancement factor F [Eq. (2)]. The magnitude of F is quite sensitive to the half-width Γ_D of the giant dipole resonance, and only approximate values of these half-widths are obtained from the (γ,n) cross-section curves. The photoneutron cross sections of Mn^{55} and Ho^{165} show a splitting of the giant dipole resonance caused by the intrinsic deformation of these nuclides. For example, high-resolution measurements^{40,41} of the (γ,n) cross section of Ho^{165} show two peaks with the

following parameters: $E_{D_1}=12.3$ MeV, $\Gamma_{D_1}=2.5$ MeV and $E_{D_2}=15.7$ MeV, $\Gamma_{D_2}=4.4$ MeV. In the calculation of F , Γ_D was taken as the sum of the two separate half-widths and E_D was taken as the average of the two peak energies.

In comparing the calculated curves with the measurements, it can be seen that the enhancement factor is needed for all of the cases, and the magnitude and shape of the calculated cross sections are in reasonable agreement with the measurements. The agreement between the calculated and measured cross sections of Na^{23} and Mn^{55} must be rather fortuitous since errors of a factor of 4 in the theoretical predictions would not be unreasonable according to Refs. 8–10. The theoretical predictions for the activation of In^{116m} and Ho^{166} have not been reduced from values given by Eqs. (1) and (2) to take into account the production of In^{116g} and Ho^{166m} .

Activation Cross Sections for the $\text{F}^{19}(n,2n)\text{F}^{18}$, $\text{Na}^{23}(n,2n)\text{Na}^{22}$, $\text{Mn}^{55}(n,2n)\text{Mn}^{54}$, $\text{In}^{115}(n,2n)\text{In}^{114m}$, $\text{Ho}^{165}(n,2n)\text{Ho}^{164m}$, $\text{In}^{115}(n,n')\text{In}^{115m}$, and $\text{Al}^{27}(n,\alpha)\text{Na}^{24}$ Reactions*

H. O. MENLOVE,[†] K. L. COOP,[‡] AND H. A. GRECH
Lockheed Palo Alto Research Laboratory, Palo Alto, California

AND

R. SHER
Stanford University, Stanford, California
 (Received 29 June 1967)

The $(n,2n)$ activation cross sections of F^{19} , Na^{23} , Mn^{55} , In^{115} , and Ho^{165} have been measured in the neutron energy range from 12.7 to 19.4 MeV. In addition, the activation cross sections for the $\text{In}^{115}(n,n')\text{In}^{115m}$ and $\text{Al}^{27}(n,\alpha)\text{Na}^{24}$ reactions have been measured in the energy range from 1.0 to 19.4 MeV and from 6.1 to 19.4 MeV, respectively. Most of the measurements were made relative to the fission cross section of U^{235} . The experimental $(n,2n)$ cross sections have been compared with the predictions of the semiempirical cross-section theories of Pearlstein and of Gardner.

INTRODUCTION

A KNOWLEDGE of the shape and magnitude of $(n,2n)$ and (n,n') cross sections as a function of neutron energy is of interest from the standpoint of nuclear-reaction theory and in connection with the use of certain materials as threshold detectors and neutron-flux-measuring standards.

In the present experiment, $(n,2n)$ activation cross sections of F^{19} , Na^{23} , Mn^{55} , In^{115} , and Ho^{165} have been

measured in the neutron energy range from 12.7 to 19.4 MeV. Also, the (n,n') activation cross section of In^{115} has been measured in the neutron energy range from 1.0 to 19.4 MeV. At most energies, all these cross sections were measured relative to the $\text{U}^{235}(n,f)$ cross section. These particular nuclides were studied since they were activated in these ways in conjunction with the (n,γ) cross-section measurements described in a companion paper.¹ In addition, the convenient decay schemes and half-lives of the product nuclides make these reactions possible candidates for use as threshold detectors. The $\text{In}^{115}(n,n')\text{In}^{115m}$ reaction is especially useful in this regard because of its low threshold (0.34 MeV) and convenient half-life (4.5 h).

* This work supported by the Lockheed Independent Research Program and is based on part of a thesis submitted by H. O. Menlove to Stanford University in partial fulfillment of the requirements for the Ph.D. degree.

[†] Present address: Los Alamos Scientific Laboratory, University of California, Los Alamos, New Mexico.

[‡] Present address: Department of Nuclear Physics, Research School of Physical Sciences, Australian National University, Canberra.

¹ H. O. Menlove, K. L. Coop, H. A. Grech, and R. Sher, *Phys. Rev.* **163**, 1308 (1967).